# Observation of the transition of operating regions in a low-pressure inductively coupled oxygen plasma by Langmuir probe measurement and optical emission spectroscopy

**Dong-cheol Seo and Tae-hun Chung**

Department of Physics, Dong-A University, Busan 604-714, Korea

**Abstract**
In inductively coupled low-pressure oxygen plasmas, planar Langmuir probes were used to determine the variation of the plasma parameters (positive and negative ion densities, electron density, electron temperature) with applied pressure (1–40 mTorr) and power (1–800 W). Simultaneous optical emission spectra were obtained. The relative abundance of the species was estimated from the intensities of the two spectral lines from excited oxygen atoms and molecular oxygen ions. In conjunction with the Langmuir probe data, the scaling behaviours of the charged and neutral species were investigated. A change of scaling behaviour in charged and neutral species densities which was due to the transition from the ion-flux-loss-dominated region to the recombination-loss-dominated region was observed by Langmuir probe measurement and optical emission spectroscopy.

## 1. Introduction

Oxygen plasmas have been used widely in various plasma processes such as the surface modification of synthetics, surface cleaning, plasma enhanced chemical vapour deposition of oxide thin films, and photoresist etching (Behle *et al* 1997, Yun and Tynan 2001). Negative ions are found in electronegative gases such as oxygen, chlorine and fluorocarbons, which are used extensively in discharges for various applications of plasma processing. The presence of negative ions complicates the discharge phenomena. There is considerable scientific and technological interest in electronegative plasmas (Lee and Lieberman 1995, Lee *et al* 1994) and so in the determination of negative-ion density (Quandt *et al* 1998, Hayashi and Kadota 1998).

The operating regions in electronegative plasmas were classified over the entire control parameter space (Lichtenberg *et al* 2000). The control parameter space is partitioned by whether the ion flux to the wall or positive–negative ion recombination is the dominant positive ion loss mechanism.

The control parameter space consists of parameters, $pL$ (pressure times system length), and $n_eL$ (electron density times system length). The discharge properties such as the ratio of the negative-ion density to the electron density, the spatial profile of charged species, and the prevailing particle loss mechanism (recombination-loss-dominated or ion-flux-loss-dominated) also depend on the operating region. Thus, in various regions, the discharge generally exhibits different scalings of the operating parameters.

In previous articles we have explored the transitions between operating regions and the scaling behaviour of inductively coupled low-pressure oxygen plasma for a low-power condition (Chung *et al* 1999) and for a medium- or high-power condition (Seo *et al* 2001) based on an electrostatic probe method. We observed that there exist transitions of the operating region from the ion-flux-loss-dominated region to the recombination-loss-dominated region with increasing operating pressure, and that experimentally measured scalings of the charged species are in agreement with the predictions of the spatially averaged global model. Because of the

complexity of the plasma sheath in the presence of negative ions, direct detection of negative ions with a Langmuir probe is difficult and needs complementary diagnostic tools. In addition, Langmuir probes are subject to contamination in oxygen, where the discharge species can react with the probe tip. The diagnostic method which is relatively reliable and broadly applicable is optical emission spectroscopy. Another concern is the scaling behaviour of the atomic oxygen. In particular, atomic oxygen plays an important role in plasma processes. Etch rates and the shapes of etched profiles depend on the relative fluxes of $O_2$, O, $O_2^+$ and $O^+$ (Yun and Tynan 2001, Mieno *et al* 1996). In a 10 mTorr ICP plasma, the predominant neutral species at low rf power is $O_2$. As rf power is increased, O radicals account for most of the neutrals. The transition from $O_2$ to O dominated plasma is smooth with almost no atomic oxygen in the capacitive mode, and increases gradually in percentage dissociation with increasing power in the inductive mode. The Langmuir probe results do not yield information about the concentrations of the reactive neutral species that are known to be important in many deposition and etching processes (Shatas *et al* 1992). Clarification of the relative abundance of O as a function of pressure and power will be made using optical emission spectroscopy.

The experiment described in this study was performed in a different type of facility compared with that employed in the previous study (Seo *et al* 2001); a low-pressure inductively coupled oxygen discharge with a different reactor geometry and wall condition. The aim of this paper is to check the existence of the operating regions and the transition between them, and to confirm that these observations are general in electronegative low-pressure discharge plasmas.

## 2. Scaling formula and transition of the operating regions

There has been an increased demand to understand the scaling of the relative abundance of $O_2$, O, $O_2^+$ and $O^+$ with control parameters such as pressure and power. Since the discharges exhibit different scaling of the operating parameters depending on the operating region where they are located, we can identify the transition of the operating regions with the change of the scaling behaviour. In this study we are restricted to a transition between the recombination-loss-dominated region and the ion-flux-loss-dominated region. A transition from the ion-flux-loss-dominated region to the recombination-loss-dominated region can be observed by increasing pressure.

The scaling relations of atomic oxygen and molecular ions are given by (Chung *et al* 1999)

$$n_O \propto \frac{n_e K_{diss} \tau_a n_{O_2}}{\gamma_{rec}}. \qquad (1)$$

For the ion-flux-loss-dominated region,

$$n_{O_2^+} \propto p^y P_{abs} \qquad (y \leqslant 1) \qquad (2)$$

and for the recombination-loss-dominated region,

$$n_{O_2^+} \propto K_{iz2} P_{abs}^{1/2}. \qquad (3)$$

Here $K_{diss}$ is the rate constant of the dissociation reaction, $n_e$ is the electron density, $\gamma_{rec}$ is the surface recombination rate,

$\tau_a$ is the confinement time of the neutral atom, $K_{iz2}$ is the rate constant of the ionization reaction, $p$ is the gas pressure and $P_{abs}$ is the absorbed power.

The neutral atom fraction increases with pressure up to a certain pressure range and then decreases slightly with pressure. With increasing pressure, $K_{diss}$ decreases and the molecule number density increases. Since $\tau_a$ is insensitive to the plasma condition, the behaviour of the density of atomic oxygen resembles that of the electron density according to (1). The positive-ion density increases with pressure in a low-pressure range and reaches a maximum, and then decreases slightly. This behaviour is related to the transition of the dominant loss mechanism of charged particles in electronegative plasmas. In a low-pressure range, the dominant loss of charged particles is due to diffusion (ion-flux-loss-dominated region), while at medium- or high-pressure ranges, the loss takes place mainly via volume recombination (including electron detachment). This region is called the recombination-loss-dominated region. The increase of volume recombination makes the charged particle density decrease with pressure.

## 3. Experimental procedure

The plasma chamber consists of a stainless steel cylinder with a diameter of 28 cm and a length of 90 cm. A 1.9 cm thick by 27 cm diameter tempered glass plate mounted on one end separates the planar one-turn induction coil from the plasma. Figure 1 shows a schematic of the planar inductive plasma source and optical emission spectroscopy system. The plasma chamber is evacuated by a turbomolecular pump (TPU 520; $520\,l\,s^{-1}$) backed by a rotary pump (DUO 30 A) giving a base pressure of $9 \times 10^{-7}$ Torr. The equilibrium gas pressure in the chamber is monitored with a combination vacuum gauge (IMG 300). The operating gas pressure is controlled adjusting the mass flow controller. The flow rate of the oxygen gas has a range of 1–60 sccm. The oxygen gas pressure is varied between 1–40 mTorr. The induction coil is made of copper and is connected to a L-type capacitive matching network and a RF amplifier (KALMUS 137C).

### 3.1. Langmuir probe

The ratio of the negative-ion density to the electron density was determined using a novel two-probe technique. The positive-ion flux (as modified by negative ions) was measured using a guard planar probe, while the negative charge saturation current was obtained using a small cylindrical probe (Chabert *et al* 1999). The negative ion concentration was then determined from the ratio of the two currents. In the present study, however, we employ a single planar probe. The details of the Langmuir probe and data acquisition system was described in a previous article (Seo *et al* 2001).

The negative-ion fraction in the bulk plasma $\alpha$ can be deduced from the saturation current ratio $R$ (Boyd and Thompson 1959, Braithwaite and Allen 1988) where

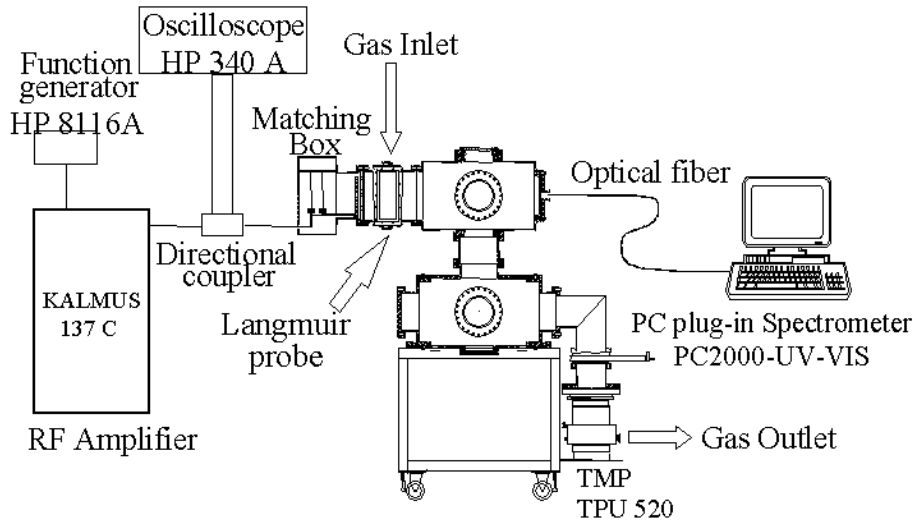$$\alpha = \frac{n_-}{n_e} \qquad R = \frac{I_S}{I_+}.$$

**Figure 1.** Schematic of an inductively coupled plasma source and diagnostics system.

The saturated current above the space potential is given by (Amemiya 1988)

$$I_S = eS\left[ n_e \left( \frac{T_e}{2\pi m} \right)^{1/2} + n_- \left( \frac{T_-}{2\pi M} \right)^{1/2} \right] \qquad (4)$$

where $e$ is the electronic charge, $S$ is the probe area, $n_e$ is the electron density, $m$ and $M$ are the masses of electrons and negative ions, respectively, $T_e$ and $T_-$ are the temperatures of the electrons and negative ions, respectively. Here the contribution of negative ions is negligible for $\alpha < 100$.

The positive ion saturation current is

$$I_+ = eS\Gamma_S(\alpha) \qquad (5)$$

where $\Gamma_S(\alpha)$ is the modified Bohm flux.

From (4) and (5), we can write

$$R \cong \left( \frac{M}{2\pi m} \right)^{1/2} \frac{n_e c_S}{\Gamma_S(\alpha)} \qquad (6)$$

where $c_S$ is the Bohm velocity.

The ratio of $T_e$ to $T_-(\approx T_+)$ is assumed to be 50. This ratio changes with plasma parameters. Stamate *et al* (2000) estimated the negative ion temperature by using a test function method for a multipolar magnetically confined oxygen plasma with pressure of 0.5–10 mTorr. The ratio was in the range of 10–50, and its dependence on the pressure and the discharge current was not significant. In the analysis of the probe data, we also consider the ratios of 10 and 100, but the choice of the value does not have a significant effect on the charged species densities either. The higher value of the temperature ratio results in larger number densities of the positive and negative ions. The temperature ratio of 100 results in about twice the positive- and negative-ion densities compared with those of the temperature ratio of 10 case. However, the negative ion temperature needs to be known accurately for the medium pressure region and cylindrical probe case (Bryant *et al* 2001). With the choice of the temperature ratio, the experimentally measured $R$ value determines the negative ion fraction based on Sheridan *et al* (1999). By measuring the slope of the probe
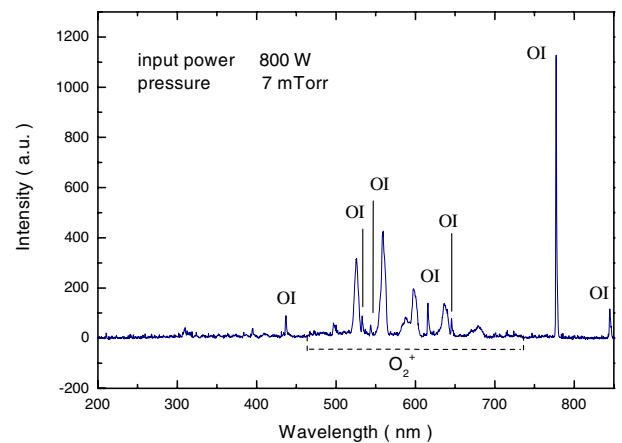


**Figure 2.** Emission spectrum of 7 mTorr, 800 W inductively coupled oxygen discharges.

$I–V$ curve one can estimate electron temperature. Equation (4) gives the electron density, and then the negative ion density. Using a density balance between negatively and positively charged particles given by $n_e + n_- = n_+$, we can obtain the positive ion density (Amemiya 1988).

### 3.2. Optical emission

The discharges are also characterized by optical emission spectroscopy. The variations of the emission line intensities are studied as a function of pressure and rf power. The optical emission experiment was performed in conjunction with the probe experiment using a 0.1 mm optical fibre which transmitted plasma emission light from a view port on the plasma chamber to the PC plug-in spectrometer. The PC2000-UV-VIS consists of a 2048-element linear CCD-array fibre optic PC plug-in spectrometer mounted on a half-length, 1 MHz ISA-bus A/D card. It is preset to a 200–850 nm wavelength range, and has a multi-bandpass order-sorting detector and a 25 mm entrance slit for high-resolution (1.5 nm FWHM) performance.
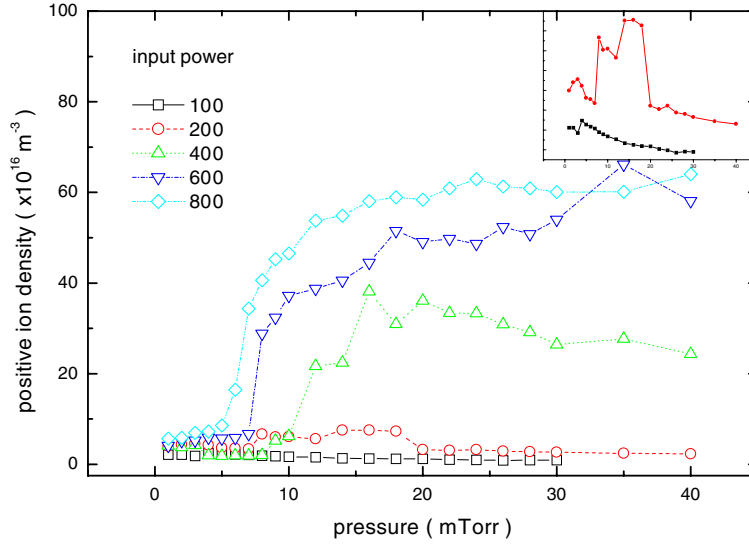
**Figure 3.** Positive-ion densities as a function of pressure for $P_{abs} = 100$–800 W. The inset shows the 100 W case (rectangles) and the 200 W case (circles).
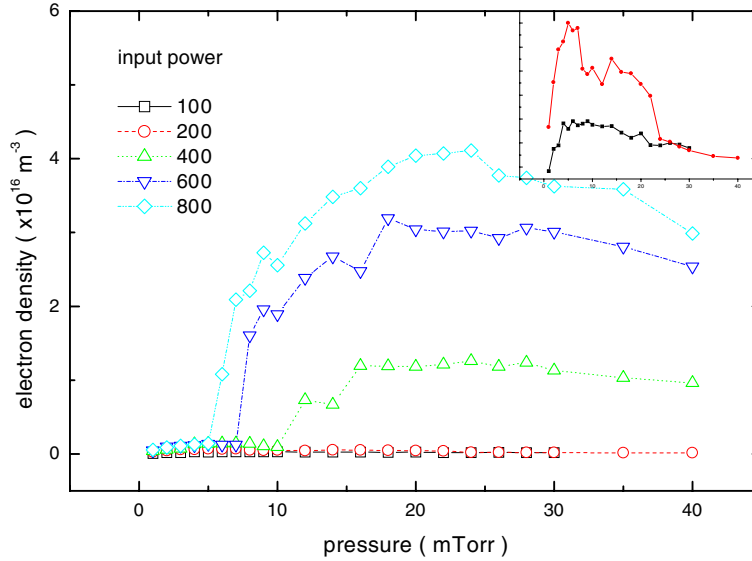


**Figure 4.** Electron density as a function of pressure for $P_{abs} = 100$–800 W. The inset shows the 100 W case (rectangles) and the 200 W case (circles).

Unlike Langmuir probe techniques, optical emission is non-invasive and is capable of detecting both neutral and ionic species. The ICP source yields a spectrum that appears to consist exclusively of $O_2^+$ bands and atomic O I lines. The spectral lines selected are O I 777.2 nm and $O_2^+$ 559.8 nm (Aoyagi *et al* 1996). Besides, atomic O I lines are seen at 394.7, 436.8, 532.9, 543.6, 615.8, 645.5 and 844.5 nm. A typical spectrum obtained with 7 mTorr oxygen and 800 W rf power is shown in figure 2.

The emission intensity of the two selected lines are given by (Sarfaty *et al* 1998)

$$I_O = C_1 n_O n_e K_{ex1} Q_1 b_{\lambda 1} \tag{7}$$

$$I_{O_2^+} = C_2 n_{O_2^+} n_e K_{ex2} Q_2 b_{\lambda 2} \tag{8}$$

$$\frac{I_O}{I_{O_2^+}} = \frac{n_O}{n_{O_2^+}} \frac{K_{ex1}}{K_{ex2}} \frac{C_1 Q_1 b_{\lambda 1}}{C_2 Q_2 b_{\lambda 2}} \tag{9}$$

where $C$ is the detector spectral response, $n$ is the ground state density of the species, $K_{ex}$ is the electron excitation rate from the ground state to the observed level, $Q$ is the quantum yield for photon emission, and $b$ is the emission branching ratio of the transition used. If the excitation energies of the neutral atom and the molecular ion are assumed to be equal and the ratio of the excitation cross sections of the neutral atom and the molecular ion to be constant in the domain of the electron energies of this experiment (Fujimura *et al* 1990), then the ratio of the number densities behaves in a similar fashion to the ratio of the emission intensities in (9).

## 4. Results and discussions

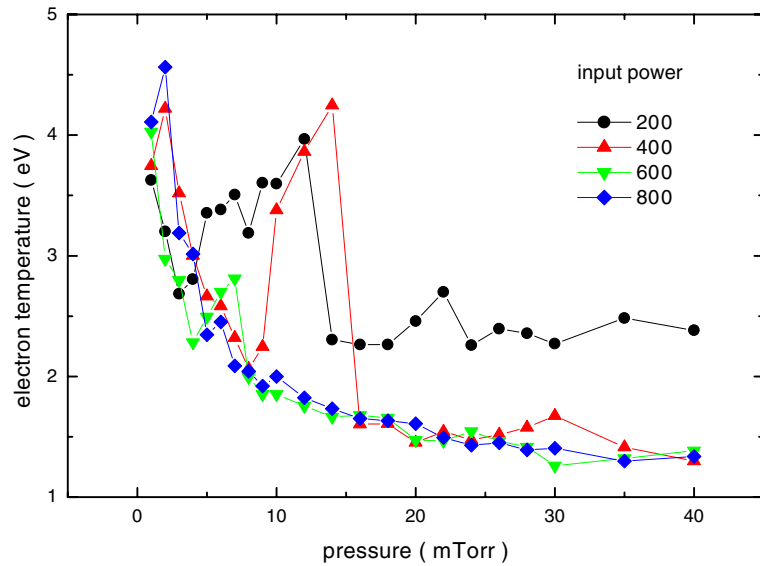Figure 3 shows the positive-ion density as a function of pressure. The variation of positive ion density with pressure

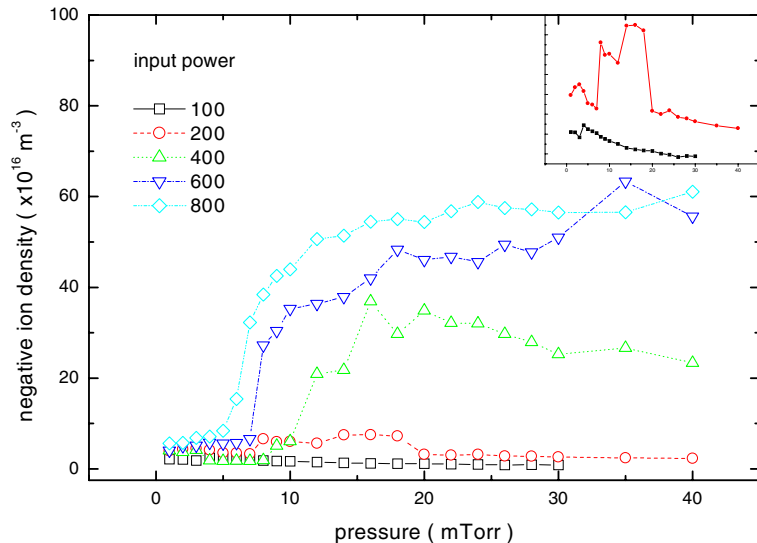**Figure 5.** Electron temperature as a function of pressure for $P_{abs} = 200$, 400, 600 and 800 W.



**Figure 6.** Negative-ion densities as a function of pressure for $P_{abs} = 1$–800 W. The inset shows the 100 W case (rectangles) and the 200 W case (circles).

is in agreement with the other experimental results (Keller *et al* 1993, Barns *et al* 1993, Ra and Chen 1993). We observe that the positive-ion density increases with pressure in a low-pressure range, and has a maximum, and then decreases slightly (input power of 100 and 200 W) or saturates (400 W and above). This behaviour seems to be related to the transition of the dominant loss mechanism of charged particles in electronegative plasmas. In the low-pressure range, the dominant loss of charged particles is due to diffusion (this region is called the ion-flux-loss-dominated region), while in the medium- or high-pressure range, the loss takes place mainly via volume recombination (the recombination-loss-dominated region). The increase of volume recombination makes the charged particle density decrease with pressure since the more charged particles a discharge produces the more recombination it results in. The increase of recombination loss along with the diffusion loss makes the charged particle density decrease or

saturate. From figure 3, we can note that the transition from the ion-flux-loss-dominated region to the recombination-loss-dominated region takes place at a specific value of pressure where the value of the charged species density has a maximum. The transition points are about 4 mTorr for 100 W inductive power, 15 mTorr for 200 W, and 35 mTorr for 600 W. The loci of the transition points can be reproduced in the pressure–power phase space from the condition, $K_{iz} = 2K_{att}$, which indicates the evenness between the volume-recombination-loss and the ion-flux-loss to the wall (Lichtenberg *et al* 2000). The transition point moves to a higher pressure value as the absorbed power increases unlike in our previous study (Seo *et al* 2001). The behaviour of the loci of the transition points also depends on the detailed plasma conditions such as the reactor geometry and the reactor wall characteristics. Until the transition point, the positive-ion density scales as in (2), after that point, it decreases according to (3).
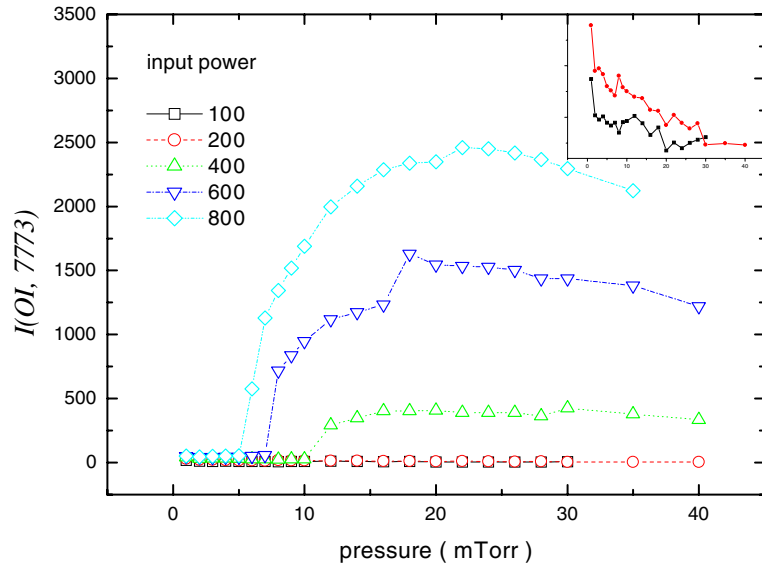
**Figure 7.** Line intensity of O I (772.2 nm) as a function of pressure for $P_{abs} = 1$–800 W. The inset shows the 100 W case (rectangles) and the 200 W case (circles).
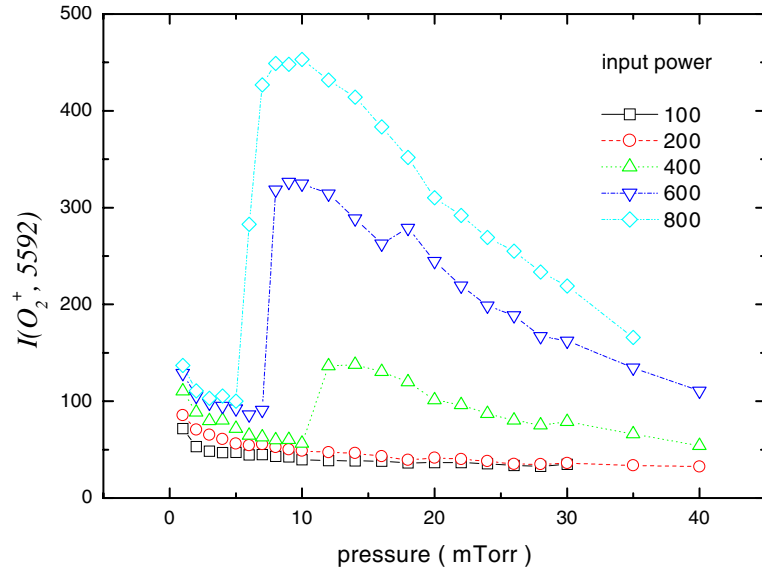


**Figure 8.** Line intensity as a function of pressure for $P_{abs} = 1$–800 W.

Figure 4 shows the electron density as a function of pressure at an input power of 100–800 W. The variation of the electron density is similar to that of the positive ion. The transition points are about 7 mTorr for 200 W inductive power, 17 mTorr for 600 W and 24 mTorr for 800 W. The transition points are shifted a little to the left compared with those of the graph for the positive ion density. Figure 5 shows the electron temperature as a function of pressure at four different powers. At the present, we have no explanation why the electron temperature is high at the low power of 200 and 400 W. The measured electron temperature ranges from 1 to 5 eV.

In figure 6, the negative-ion density is shown as a function of pressure with varying absorbed power. The variation of the negative-ion density is similar to that of the positive ion. The similar dependence of the negative-ion density on pressure has been observed regardless of the operating pressure regime and

the discharge mechanism in the experiments of Hebner and Miller (2000), Ra *et al* (1994), Stoffels *et al* (1995), and in the pulsed mode calculation of Panda *et al* (2000). The results for the low-pressure region are qualitatively consistent with the experimental results by Tuszewski (1996) and Gudmundsson (1996).

The deviation between the predictions of the scaling formulas and the experimental results originate from the fact that the scaling relations are derived based on a simple-minded global balance and that the experimental results are obtained by a single Langmuir probe. The probe technique has some drawbacks in applying to electronegative plasma since it is difficult to get both the positive ion saturation current and the negative charge saturation current with a single probe due to the difference in the sheath area of the charge collection (Chabert *et al* 1999). The probe method is usually applicable when the
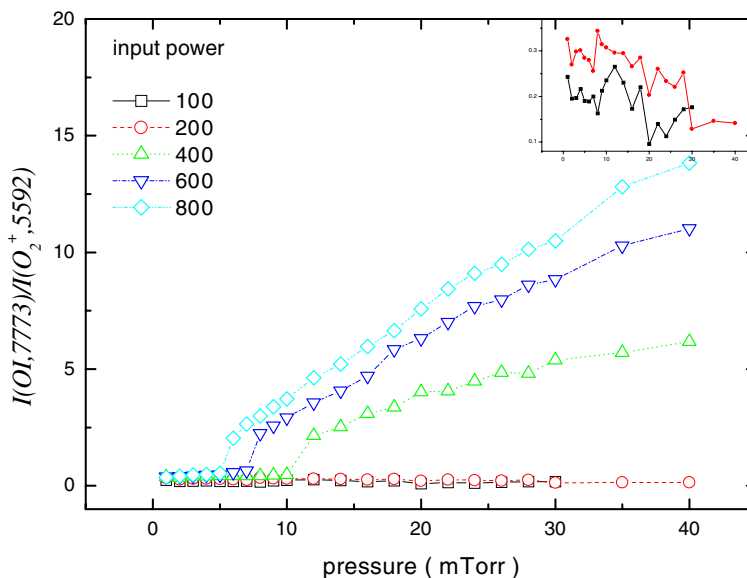
**Figure 9.** Intensity ratio as a function of pressure for $P_{abs} = 1$–800 W. The inset shows the 100 W case (rectangles) and the 200 W case (circles).

density ratio of negative ions to electrons is large. However, the method can be extended to the case of a small ratio of negative ions by utilizing the second derivative of the probe characteristics (Vucelic and Mijovic 1998).

Figure 7 shows the intensity at 777.2 nm as a function of pressure for five different powers. The variation of the emission intensity with pressure and power resembles that of the electron density. At the powers of 100 and 200 W, the intensity decreases with pressure. On the other hand, at 400 W and above, the degree of dissociation of the oxygen molecules becomes quite high, and the line intensity shows a different scaling with pressure. The increase of the line intensity accounts for an increase of the excited oxygen atom. The abundance of the excited oxygen atom is closely related to the abundance of the electron density except at the lower pressure region (below 10 mTorr). This can be accounted for by the scaling formula (1). In addition to the electron impact excitation of the ground state oxygen atom, the mutual recombination of $O^+$ and $O^-$ leads to the excited oxygen atom which emits O I line (Ishikawa *et al* 1998). The diversity of routes in generating the excited oxygen atom makes the excited atom density increase at a certain range where negative ions are abundant. This phenomenon is related to the transition of the operating region. The transition from the ion-flux-loss-dominated region to the recombination-loss-dominated region takes place around 17 mTorr for 600 W power and 24 mTorr for the 800 W case. The transition points roughly coincide with those of the graph for the electron density.

In figure 8, the variation of the emission line intensity from the molecular oxygen ion at 559.2 nm with pressure and power is shown. Above the power of 400 W, the emission intensities become large and have peaks at specific pressures. The decrease of the intensity with increasing pressure is related to the scaling behaviour of the positive ion with pressure. The intensity ratio is proportional to the density ratio of O and $O_2^+$ provided that $K_{ex}$, $C$, $Q$ and $b$ are not sensitive to the electron temperature (which depends on the pressure and

power). From figure 9, we observe that the transition occurs around 8 mTorr where the scaling changed abruptly. The reason for the discrepancy in the location of the transition point with that in the graph of the charged species density is that the ratio of $K_{ex}$ is influenced by the plasma condition. As can be expected from the scaling formula, the intensity ratio has a linear dependence on power above the transition and the ratio increases with pressure in the recombination-loss-dominated region.

## 5. Conclusion

The transitions from the ion-flux-loss-dominated region to the recombination-loss-dominated region were observed by Langmuir probe measurement and optical emission spectroscopy. The transition point moves to higher pressures as the absorbed power increases. Each region has a different scaling of plasma variables, which proves to be in good qualitative agreement with the predictions of the global model. It was found that inductively coupled low-pressure oxygen discharges are highly dissociated at a specific pressure region and at high powers. The abundance of the excited oxygen atom is closely related to the abundance of the electron density except at the lower pressure region (below 10 mTorr). In the future we hope to obtain the absolute densities of species from optical measurement actinometry.

## Acknowledgments

## References

Aoyagi K, Ishikawa I, Saito Y and Suganomata S 1996 *Japan. J. Appl. Phys.* **35** 6248

Amemiya H 1988 *J. Phys. Soc. Japan* **57** 887

Barns M S, Forster J C and Keller J H 1993 *Appl. Phys. Lett.* **62** 2622

Behle St, Georg A, Yuan Y, Engemann J and Brockhaus A 1997 *Surf. Coat. Technol.* **97** 734

Boyd R L F and Thomson J B 1959 *Proc. R. Soc.* A **252** 102

Braithwait N St J and Allen J E 1988 *J. Phys. D: Appl. Phys.* **21** 1733

Bryant P, Dyson A and Allen J E 2001 *J. Phys. D: Appl. Phys.* **34** 95

Chabert P, Sheridan T E, Boswell R W and Perrins J 1999 *Plasma Sources Sci. Technol.* **8** 561

Chung T H, Yoon H J and Seo D C 1999 *J. Appl. Phys.* **86** 3536

Fujimura S, Shinagawa K, Nakamura M and Yano H 1990 *Japan. J. Appl. Phys.* **29** 2165

Gudmundsson J T 1996 *PhD Thesis* University of California at Berkeley

Hayashi D and Kadota K 1998 *J. Appl. Phys.* **83** 697

Hebner G A and Miller P A 2000 *J. Appl. Phys.* **87** 7660

Ishikawa T, Hayashi D, Sasaki K and Kadota K 1998 *Appl. Phys. Lett.* **72** 2391

Keller J H, Forster J C, and Barns M S 1993 *J. Vac. Sci. Technol.* A **11** 2487

Lee C and Lieberman M A 1995 *J. Vac. Sci. Technol.* A **13** 368

Lee C, Graves D B, Lieberman M A and Hess D W 1994 *J. Electrochem. Soc.* **141** 1546

Lichtenberg A J, Lieberman M A, Kouznetsov I G and Chung T H 2000 *Plasma Sources Sci. Technol.* **9** 45

Mieno T, Kamo T, Hayashi D, Shoji T and Kadota K 1996 *Appl. Phys. Lett.* **69** 61

Panda S, Economou D J and Meyyappan M 2000 *J. Appl. Phys.* **87** 8323

Quandt E, Dobele H F and Graham W G 1998 *Appl. Phys. Lett.* **72** 2394

Ra Y and Chen C H 1993 *J. Vac. Sci. Technol.* A **11** 2911

Ra Y, Bradly S G and Chen C H 1994 *J. Vac. Sci. Technol.* A **12** 1328

Sarfaty M, Harper M and Hershkowitz N 1998 *Rev. Sci. Instrum.* **69** 3176

Seo D C, Chung T H, Yoon H J and Kim G H 2001 *J. Appl. Phys.* **89** 4218

Shatas A A, Hu Y Z and Irene E A 1992 *J. Vac. Sci. Technol.* A **10** 3119

Sheridon T E, Chabert P and Boswell R W 1999 *Plasma Sources Sci. Technol.* **8** 457

Stamate E, Kimura T and Ohe K 2000 *Proc. 17th Symp. Plasma Processing (Division of Plasma Electronics, The Japan Society of Applied Physics)* p 259

Stoffels E, Stoffels W W, Vender D, Kando M, Kroesen G M W and de Hoog F J 1995 *Phys. Rev.* E **51** 2425

Tuszewski M 1996 *J. Appl. Phys.* **79** 8967

Vucelic M and Mijovic S 1998 *J. Appl. Phys.* **84** 4731

Yun S and Tynan G R 2001 *J. Appl. Phys.* **89** 911